

Supporting Information for

Tuning Charge Generation Process of Rylene Imide-Based Solar Cells via Chalcogen-Atom-Annulation

Ningning Liang,[†] Xixiang Zhu,^{§,||} Zhong Zheng,[⊥] Dong Meng,[‡] Guogang Liu,[‡] Jianqi Zhang,[⊥] Sunsun Li,[‡] Yan Li,[‡] Jianhui Hou,^{*,‡} Bin Hu,^{*,||} Zhaohui Wang^{*,†}

[†]Key Laboratory of Organic Optoelectronics and Molecular Engineering, Department of Chemistry, Tsinghua University, Beijing 100084, P. R. China

[‡]Beijing National Laboratory for Molecular Sciences, State Key Laboratory of Polymer Physics and Chemistry, Institute of Chemistry, Chinese Academy of Sciences, Beijing 100190, P. R. China

[§]Key Laboratory of Luminescence and Optical Information, Ministry of Education, School of Science, Beijing Jiaotong University, Beijing 100044, P. R. China

^{||}Department of Materials Science and Engineering, University of Tennessee, Knoxville, TN 37996, USA

[⊥]National Center for Nanoscience and Technology, Beijing 100190, P. R. China

Table of Contents

Materials	S2
Experimental Section	S2
1. X-ray photoelectron spectroscopy (XPS) measurement	S2
2. Devices Fabrication and Characterization	S3
3. Optical-electronic properties of TPH and TPH-Se	S4
4. Devices Characterization	S5

Materials

PBDB-TF, TPH and TPH-Se were synthesized according to the relevant literature. The chemical structures are as follows:

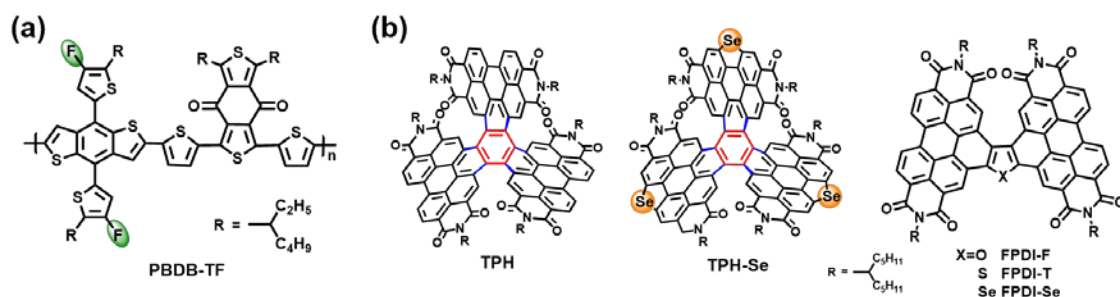


Figure S1. Chemical structure of (a) donor PBDB-TF; (b) acceptor materials, TPH, TPH-Se and FPDl-F, FPDl-T, FPDl-Se.

Experimental Section

1. X-ray photoelectron spectroscopy (XPS) measurement

XPS spectra of the TPH, TPH-Se, PBDB-TF neat films and PBDB-TF:TPH, PBDB-TF:TPH-Se blend films were recorded using ESCALab220i-XL with bichromatic Al K α (Excitation energy of 1486.6 eV) and Mg K α (Excitation energy of 1253.6 eV) as an excitation source. All of the films were spin-coated on the 10 mm \times 10 mm Si substrate.

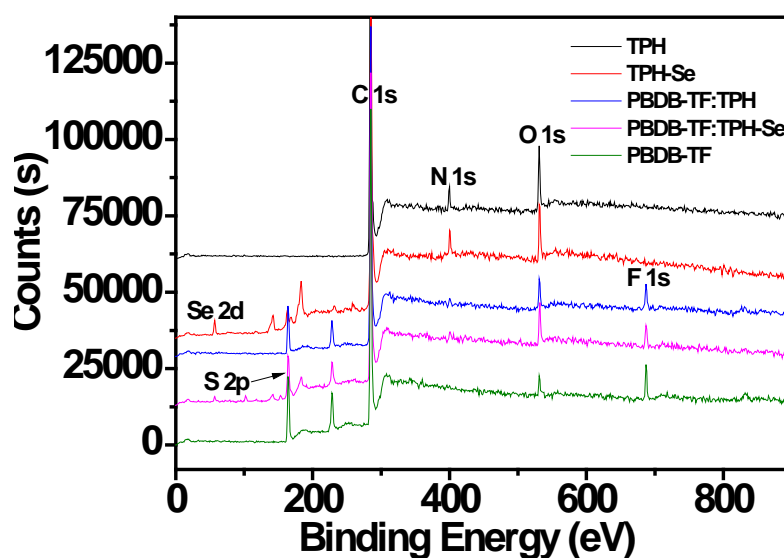


Figure S2. XPS survey of neat and blend films.

2. Devices Fabrication and Characterization

(1) Preparation of ZnO cathode buffer layer: The ITO-coated glass ($15 \Omega/\square$) was cleaned with deionized water, acetone, and isopropanol, respectively, in an ultrasonic bath. The precursor solution of ZnO was combined 0.5 M zinc acetate dihydrate and 0.5 M ethanolamine in 2-methoxyethanol and stirred at room temperature until the solvent was completely dissolved. Then the precursor solution was spin-coated onto the ITO substrate after UV/ozone cleaning for 20 min to obtain a buffer layer with a thickness of 40 nm. Following, the substrates were dried by baking in an oven at 200 °C for 60 min in air.

(2) Preparation of photoactive layers: At first, the blend of donor and acceptor materials was solved into chlorobenzene (CB) solution with 10 mg/mL of polymers and stirred at 50 °C for at least 5 hours. The active layer of four type of solutions with different D:A ratio and different volume of DIO was then deposited on top of the ZnO layer by spin-coating for about 85-nm-thick active layers.

(3) Device fabrication: Following by the thermal annealing with different temperature for 20 mins and then thermally evaporated 10-nm-thick MoO_x as the anode buffer layer under vacuum at a pressure of 3×10^{-4} Pa. Finally, 100-nm-thick Al layer was evaporated on top of the active layer. The effective area, namely the overlapping area between the cathode and anode was measured as about 0.04 cm².

(4) Device measurement: The $J-V$ characteristic was performed via the solar simulator (SS-F5-3A, Enlitech) along with AM 1.5G spectra whose light-intensity was calibrated by the certified standard silicon solar cell (SRC-2020, Enlitech) at 100 mW/cm². The EQE data were obtained from a solar cell spectral response measurement system (QE-R3011, Enli Technology Co. Ltd). Meanwhile, the film thickness was measured via a surface profilometer (Dektak XT, Bruker).

Table S1. Photovoltaic Parameters of the solar cells based on PBDB-TF:TPH and PBDB-TF:TPH-Se at different conditions under AM 1.5G illumination of 100 mW/cm²

Active layer	Condition	V_{oc} (V)	J_{sc} (mA/cm ²)	FF	PCE (%)	PCE (best) (%)
PBDB-TF:TPH-Se	1.5:1	1.04±0.004	13.53±0.34	0.578±0.001	8.15±0.17	8.44
	1.25:1	1.04±0.004	13.83±0.24	0.613±0.01	8.85±0.08	8.94
	1:1	1.05±0.003	13.92±0.21	0.619±0.01	9.09±0.14	9.28
	0.5% DIO+130 °C	1.05±0.007	14.00±0.36	0.638±0.01	9.37±0.32	9.63
PBDB-TF:TPH	1:1.25	1.04±0.006	13.00±0.39	0.599±0.02	8.11±0.08	8.24
	1:1	1.04±0.002	12.98±0.32	0.587±0.01	7.90±0.14	8.04
	0.5% DIO+130 °C	1.04±0.001	13.15±0.28	0.620±0.03	8.48±0.16	8.65

3. Optical-electronic properties of TPH and TPH-Se

Cyclic voltammograms (CV) were recorded on a Zahner IM6e electrochemical workstation using glassy carbon discs as the working electrode, Pt wire as the counter electrode, Ag/AgCl electrode as the reference electrode at a scanning rate of 100 mV/s. 0.1 M Bu₄NPF₆ (tetrabutylammoniumhexafluorophosphate) was dissolved in acetonitrile, which was calibrated by the ferrocene/ferricenium (Fc/Fc⁺) as the redox couple. All of the thin films were deposited from CHCl₃ solution onto the working electrode. Ultraviolet–visible (UV–vis) absorption spectra of acceptors in dilute CB at different concentration and different temperature as well as in solid film were measured with a Hitachi (Model U-3010) spectrophotometer in a 1-cm quartz cell.

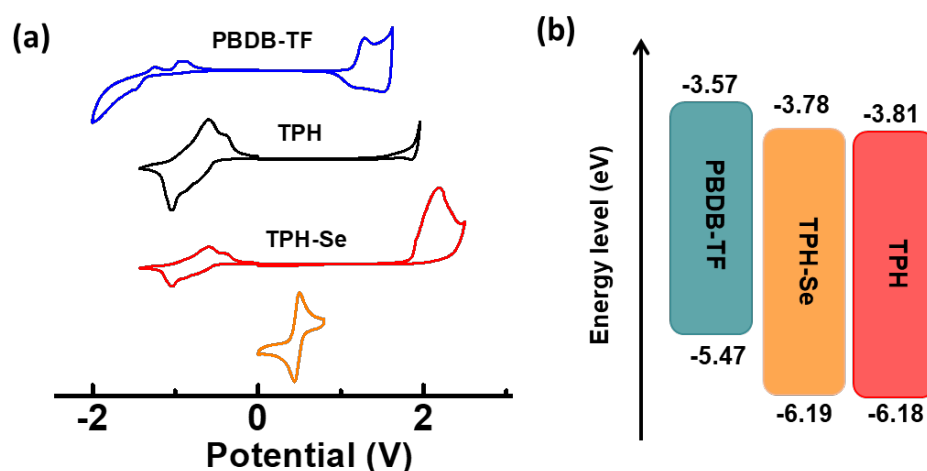


Figure S3. (a) Cyclic voltammetry plot of donor material and acceptor materials in films; (b) Energy level diagram of donor and acceptor materials.

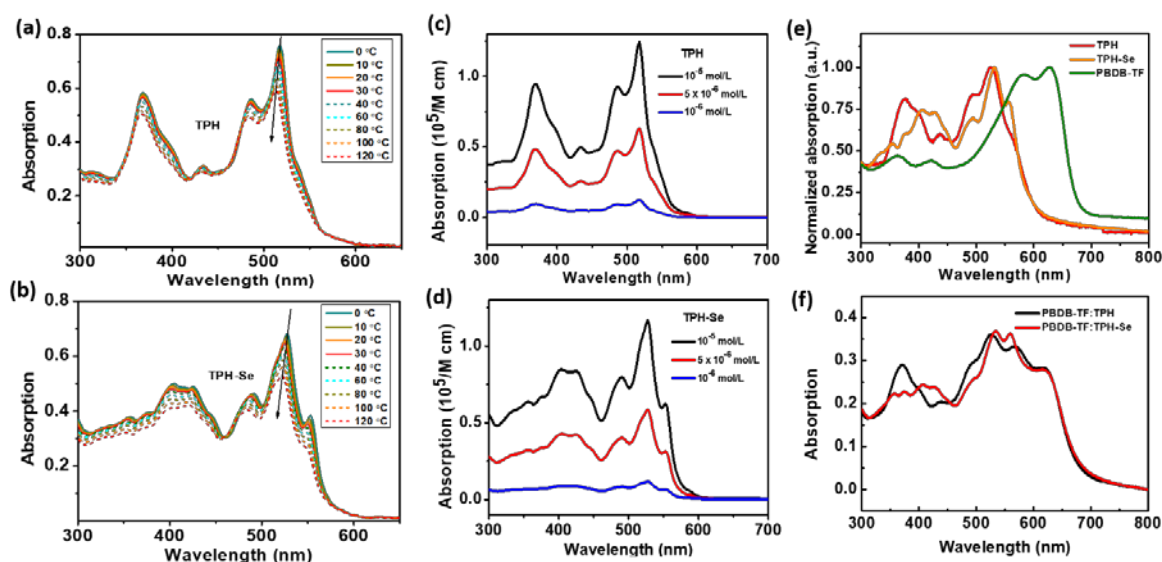


Figure S4. Absorption spectra of TPH (a) and TPH-Se (b) in dilute CB (5×10^{-5} mol/L) at different temperature; Absorption spectra of TPH (c) and TPH-Se (d) in dilute CB with different concentration; (e) UV-Vis absorption spectra of TPH, TPH-Se and PBDB-TF thin films; (f) Absorption of ZnO/blend film fabricated under optimal conditions.

4. Devices Characterization

AFM measurement were performed via a Nanoscope V AFM in tapping mode. In addition, the model of Source Measure Unit is Keithley 2450. GIWAXS and GISAXS data were obtained on a XEUSS SAXS/WAXS SYSTEM (XENOCOS, FRANCE) at the National Center for Nanoscience and Technology (NCNST, Beijing).

FTPS-EQE was performed using a Vertex 70 from Bruker optics, equipped with a QTH lamp, quartz beamsplitter and external detector option. SR570, a low noise current amplifier, is used to amplify the photocurrent of the solar cell devices with light modulated by FTIR. In order to be able to use the FTIR's software to collect the photocurrent spectrum, the output voltage of the current amplifier is fed back into the external detector port of the FTIR.

In Magnetic-field effect (MFE) measurement, the class IIIB laser product (Changchun New Industries Optoelectronics Tech CO., Ltd) with the laser of 532 nm and a light density of 46.5 mW/cm^2 . The laser of 532 nm was used in order to excite the PDI acceptors. The light density of 46.5 mW/cm^2 of this laser product is performed to generate the similar photocurrent density with that of solar simulator (SS-F5-3A, Enlitech) along with AM 1.5G spectra.

Fluorescence quantum yields of the neat TPH, TPH-Se films and PBDB-TF:TPH, PBDB-TF:TPH-Se blend films were determined by FLS980 fluorimeter at room temperature. The neat films were spin-coated from CB solution with a concentration of 15 mg/mL with a thickness of 50 nm. The blend films were fabricated under optimized condition for the best devices onto $1 \text{ cm} \times 1 \text{ cm}$ quartz tablets. The excitation wavelength was controlled by software-controlled monochromator and the absolute quantum yields were obtained in real time by the multichannel detectors. The excitation wavelength of 480 nm was selected to excite the pure acceptor films, in view of their maximum absorption peaks are located at 490~550 nm. This wavelength could also excite the PBDB-TF film. Therefore, the wavelength of 620 nm was selected to excite the blend films and the PLQY values were obtained from the average of five values.

Photo-CELIV measurements were performed by the all-in-one characterization platform Paios developed and commercialized by Fluxim AG, Switzerland.

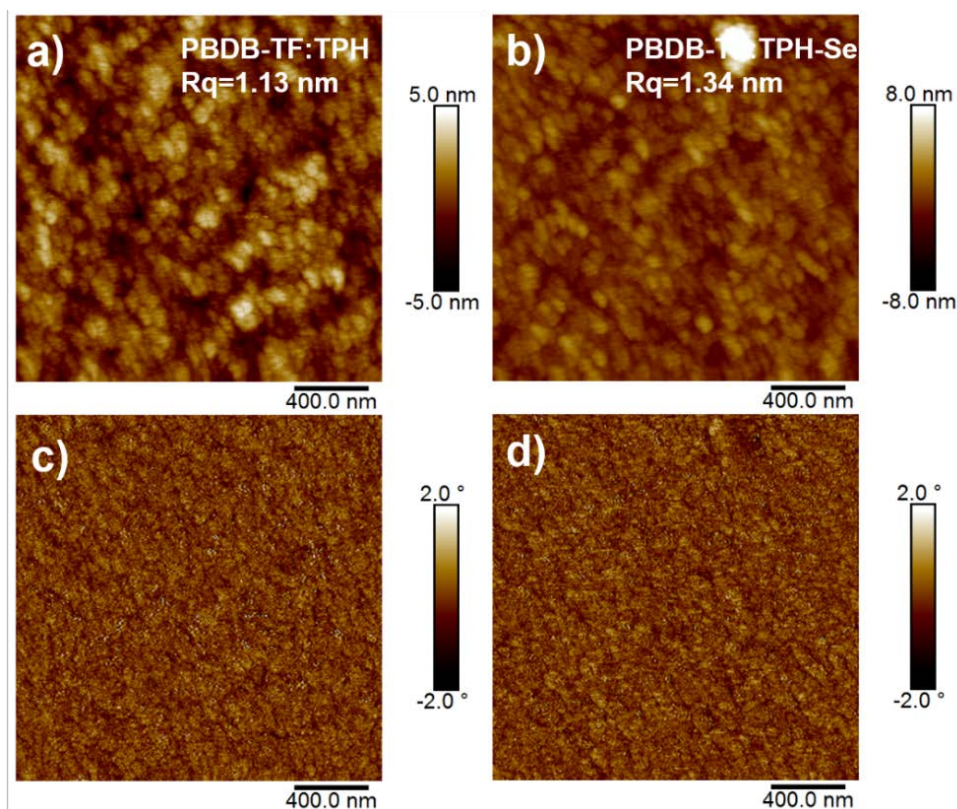


Figure S5. (a), (b) AFM height images and (c), (d) phase images of PBDB-TF:TPH and PBDB-TF:TPH-Se blend films.

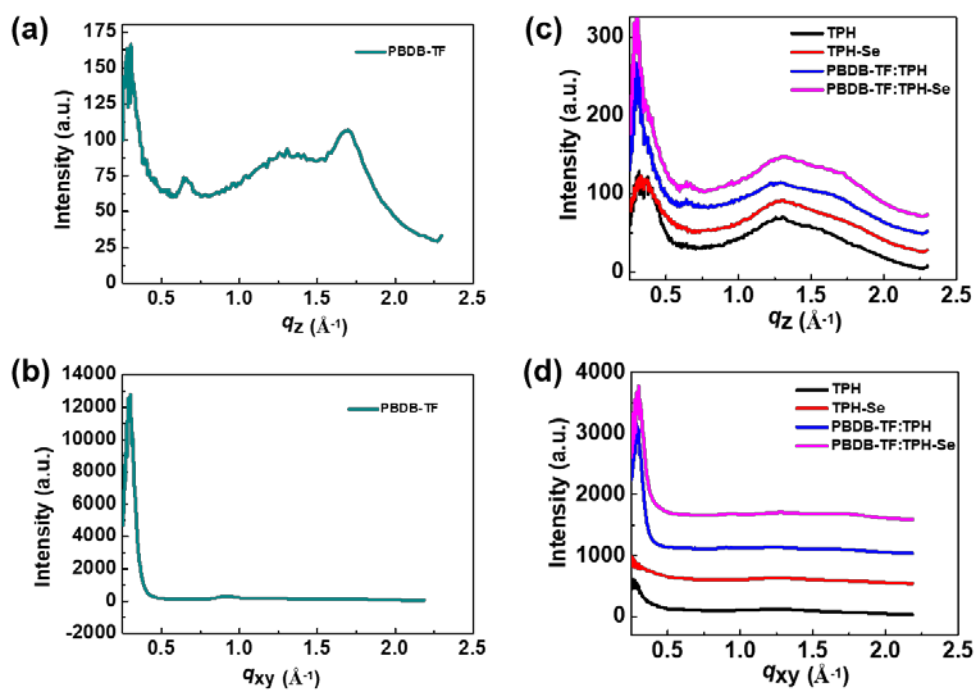


Figure S6. (a) Out-of-plane and (b) in-plane cuts of the GIWAXS patterns for PBDB-TF films; (c) Out-of-plane and (d) in-plane cuts of the GIWAXS patterns for the TPH, TPH-Se, PBDB-TF:TPH and PBDB-TF:TPH-Se films.

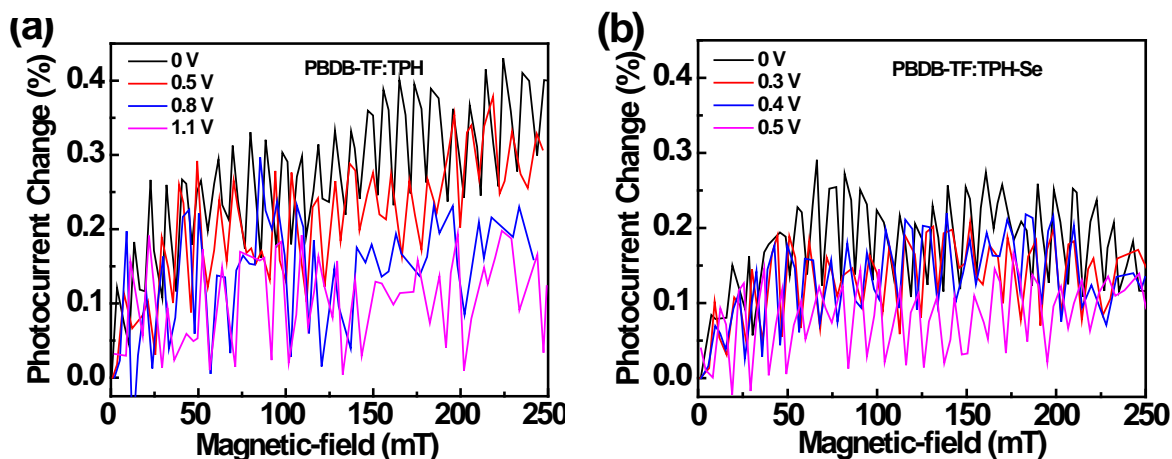


Figure S7. Photocurrent change for PBDB-TF:TPH and PBDB-TF:TPH-Se based devices at different reverse bias voltage.

Table S2. The absolute quantum yield of neat and blend films

Sample	$\phi_{\text{H}}^{(a)}$	$\phi_{\text{H}}^{(b)}$
TPH film	4.35%	—
TPH-Se film	1.79%	—
PBDB-TF film	—	2.16%
PBDB-TF:TPH film	—	0.59%
PBDB-TF:TPH-Se film	—	0.29%

^(a) Excite @ 480 nm; ^(b) Excite @ 620 nm

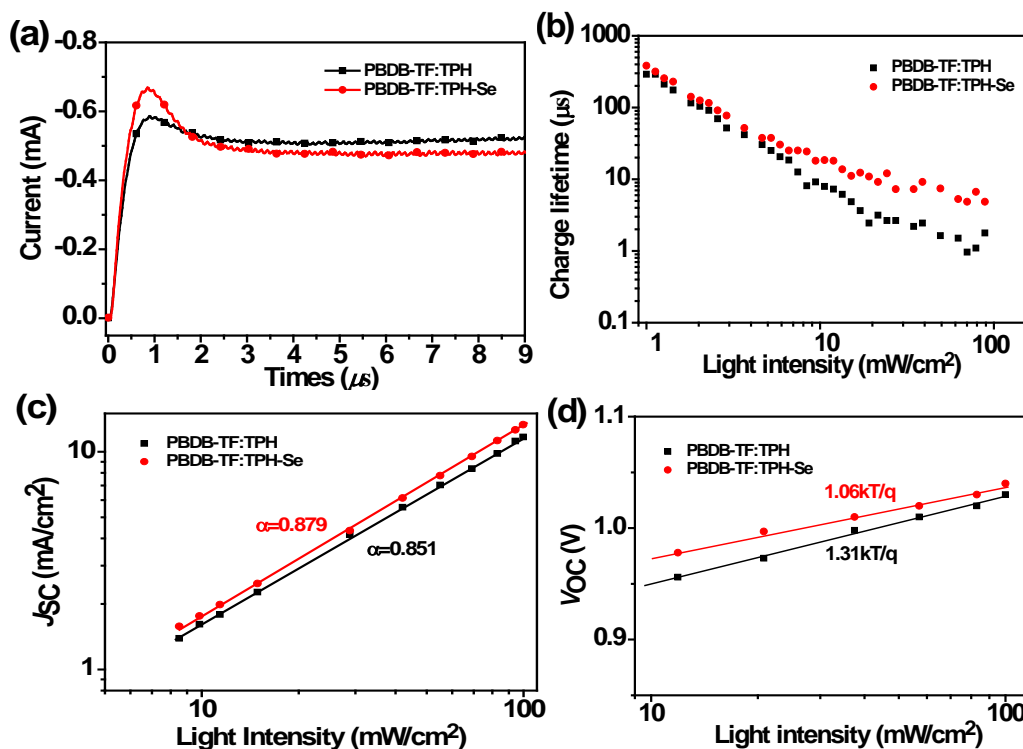


Figure S8. (a) Photo-CELIV transients recorded at the delay time of 3 ms with a ramp rate 215 V/ms; (b) charge-carrier lifetime as a function of light intensity; (c) plots of J_{sc} versus light intensities and (d) plots of V_{oc} versus light intensities for PBDB-TF:TPH and PBDB-TF:TPH-Se devices.

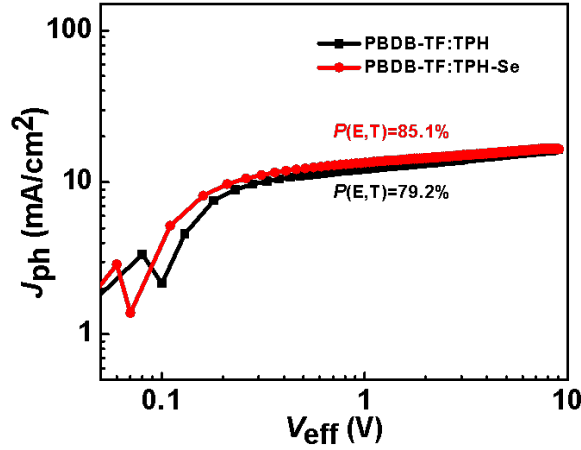


Figure S9. J_{ph} as a function of V_{eff} characteristics of solar cells based on different active layers processed at optimal condition.

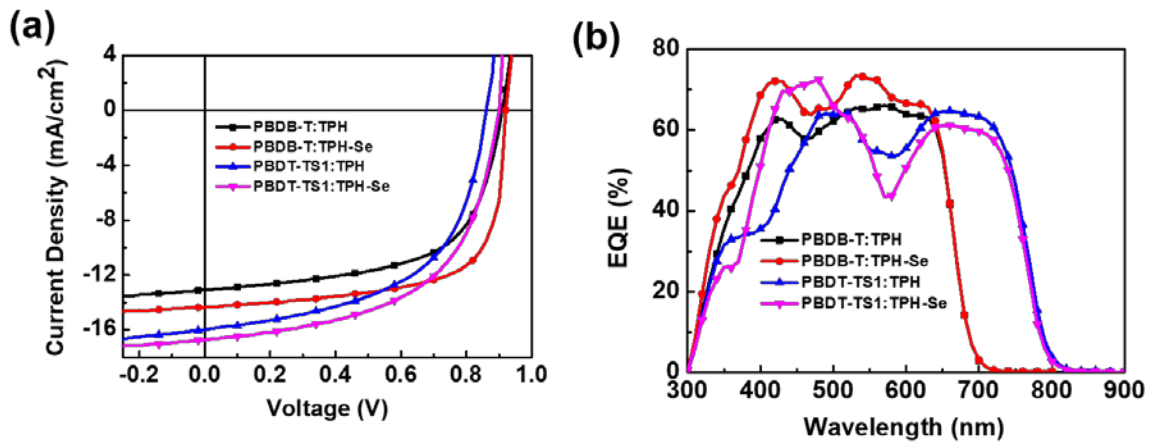


Figure S10. (a) J - V curves and (b) EQE characteristics of PBDB-T:TPH, PBDB-T:TPH-Se, PBDT-TS1:TPH and PBDT-TS1:TPH-Se based solar cells.

Table S3. Photovoltaic parameters of the solar cells based on different active layers at optimal condition under AM 1.5G illumination of 100 mW/cm^2

Active layer	D/A	Condition	V_{oc} (V)	J_{sc} (mA/cm^2)	FF	PCE (%)	PCE (best) (%)
PBDB-T:TPH	1.5:1	CB+0.5% DIO 130 °C for 10 min	0.906 ± 0.004	12.02 ± 0.09	0.688 ± 0.005	7.60 ± 0.18	7.97
PBDB-T:TPH-Se	1.25:1	CB+0.5% DIO 130 °C for 10 min	0.939 ± 0.003	13.41 ± 0.11	0.704 ± 0.005	8.87 ± 0.11	9.05
PBDT-TS1:TPH	1:1	CB+0.5% DPE	0.857 ± 0.003	15.92 ± 0.25	0.545 ± 0.007	7.44 ± 0.09	7.60
PBDT-TS1:TPH-Se	1:1	CB+0.5% DPE	0.903 ± 0.036	16.53 ± 0.26	0.555 ± 0.008	8.22 ± 0.12	8.52